The onset of nucleate boiling of self-rewetting fluids in microchannels

A Sitar[1,3], M Zupančič[1], M Crivellari[2] and I Golobič[1]

[1]University of Ljubljana, Faculty of Mechanical Engineering, Aškerčeva 6, 1000 Ljubljana, Slovenia
[2]Fondazione Bruno Kessler, Center for Materials and Microsystems, Via Sommarive 18, I - 38123 Povo, Trento, Italy

E-mail: anze.sitar@fs.uni-lj.si

Abstract. The comparative experimental analysis of flow boiling of pure water and four different self-rewetting fluids (6% butanol, 2% pentanol, 0.6% hexanol and 0.15% heptanol aqueous solution) was performed in an array of interconnected 50×50 μm microchannels. The results show that the onset of boiling was postponed to higher surface superheats when SRFs were used instead of water. In addition, the visualization of the flow boiling of self-rewetting fluids showed a substantially more abrupt and unstable flow, which was observed as a misty two-phase flow in the microchannel array. Both occurrences are attributable to (i) the absence of properly sized nucleation cavities in the microchannels and (ii) higher achieved temperatures during boiling of self-rewetting fluids, which lead to a higher momentum force of the emerging vapor phase. The measured static and dynamic contact angles and therefore also the surface tension of the used self-rewetting fluids are lower in comparison with water.

1. Introduction

Flow boiling in larger channels as well as in microchannels introduces some advantages compared to the single-phase flow: improved heat transfer coefficient, more uniform temperature distribution, smaller mass flux required, etc. However, there are also some drawbacks of employing boiling in microchannels, which are extensively described in the literature: flow instabilities [1], high superheats required for the ONB [2], vapor backflows [3,4]. One of the possible methods of the boiling heat transfer enhancement is the improvement of the channels' construction (nucleation sites [5], fins and other surface improvements [6], constructional theory designs [7]), whereas the use of an appropriate working fluid presents a simpler and an inexpensive way of increasing the heat transfer performance of an existent heat transfer device. It is difficult to substitute water in an attempt to improve the heat transfer coefficient during boiling, due to its' large latent heat. However, the use of the so-called self-rewetting fluids (SRF) already confirmed some benefits over water. The most distinguishing thermodynamic property of the SRFs is the increasing surface tension at increasing temperature, which is a unique and highly beneficial quality. Namely, SRF used as the working fluid promotes faster wetting of the hot and dried spots, which inevitably occur during boiling [8].

The self-rewetting property relies on the Marangoni effect and the positive surface tension gradient at increasing temperatures, which was presented in Savino *et al* [9] for butanol and heptanol aqueous solution along with some ternary mixtures. The performance of a heat pipe was improved in Senthilkumar *et al* [10] by adding n-butanol and especially n-pentanol to water. Authors claim that the

SRF showed a more stable and higher thermal efficiency and also lower thermal resistance compared to the experiments conducted with water as the working fluid. The comparison of the heat transfer performance of a loop heat pipe using various concentrations of three different alcohols (butanol, pentanol and hexanol) in water was presented by Wu [11]. The experimental results indicated that the optimal SRF for the heat transfer in a heat pipe at the selected working conditions was a 6 % aqueous butanol solution. Another experimental investigation of the SRF heat transfer in heat pipes was presented in Su *et al* [12], where a combination of n-butanol aqueous solution and graphene oxide nanofluid was used. Authors demonstrated a 16 % improvement in the heat transfer performance with the addition of an optimal amount of the nanofluid to the SRF, compared to the heat transfer performance of the SRF alone.

Other researchers have focused on enhancing the heat transfer in pool boiling, which is more similar to flow boiling in microchannels compared to the heat transfer in heat pipes. Recently, Hu et al. [13,14] improved the heat transfer during pool boiling of heptanol-water mixture and attributed the enhancement to: (i) the accelerated wetting of the dried spots, due to the reversed Marangoni effect (positive surface tension gradient), (ii) the more difficult coalescence of the emerging bubbles, (iii) thicker liquid layer on the heated area and (iv) smaller bubbles formation on the heater (micro-bubble emission). Zhou *et al* [15] performed pool boiling experiments with aqueous solutions of butanol, pentanol and hexanol with the mass concentrations of 7.3%, 2.2%, and 0.6%, respectively. The authors showed that with increasing the alcohols' molecular weight, the heat transfer during boiling also enhances.

The transition of SRF to a microcavity was presented in a numerical study by Zhou *et al* [16] with using a n-butanol aqueous solution. The results show that the heat transfer of the employed SRF is superior to water. Experimental investigation of a n-butanol solution in a microchannel flow boiling was presented in Sitar and Golobič [17]. The SRF provided a 10 K decrease of the maximum temperature compared to the pure water boiling at the same heat flux. Additional publications of SRF in microchannels were not found in the open literature. Therefore, our current study aims to disclose the effects of various self-rewetting fluids on boiling in microchannels. We are focused on four alcohol-water binary mixtures with a known positive surface gradient, which promotes the Marangoni flow of the liquid to the dried-out areas.

2. Materials and methods

2.1. Experimental setup and measurement procedure

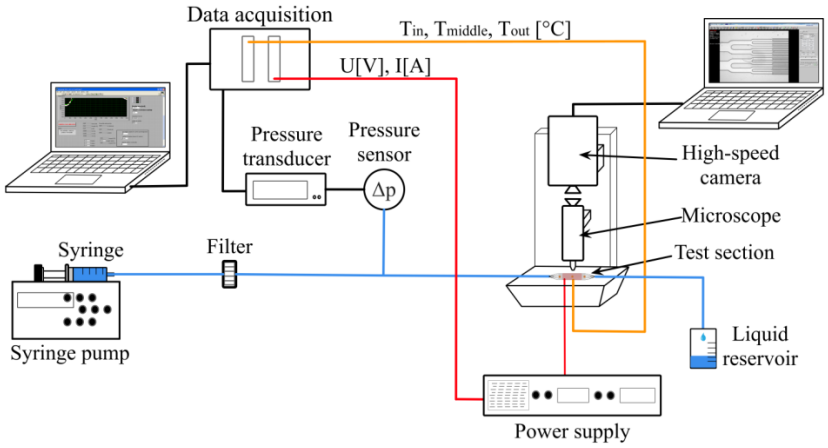

Figure 1. Experimental setup.

The experimental setup was comprised of a visualization system and a measuring system as presented

in figure 1. Temperatures were measured at three locations with a Pt100 class A resistive temperature detectors with an accuracy of 0.35°C at 100°C. Pressure was determined with a Validyne DP15 sensor, which was connected to the pressure transducer. Voltage drop across the heater elements was measured directly with the data acquisition system, whereas the electrical current was determined indirectly with a voltage drop measurement on a reference shunt with a 0.05 Ω resistance. A detailed description of the used experimental setup is available in Sitar *et al* [18].

The comparative analysis of the different working fluids is substantially affected by the operating conditions of the heat transfer experiments. The heat losses and the temperatures of the surrounding air and surfaces have an important impact on the measured temperatures during the boiling experiments. Considering these influential parameters, we utilized the same heating procedure for all of the conducted experiments (e.g. see table 1). The only controlled quantity was the heater's voltage, whereas all the following parameter values are approximate and vary a little from one to another experimental run. The subordinate quantities depend on the applied voltage and also on the heaters' temperature, which affects its electrical resistance and consequentially also the electrical current as well as the heating power.

Table 1. Power supply heating cycle and heater characteristics.

Time (min)	**Electrical voltage (V)**	**Heating power (W)**	**Electrical current (A)**	**Heater's electrical resistance (Ω)**
0	0	0	0.0	-
1.5	1	0.3	0.3	3.3
3	2	1.0	0.5	4.0
4.5	3	2.2	0.7	4.1
6	4	3.7	0.9	4.3
7.5	5	5.6	1.1	4.5
9	6	7.6	1.3	4.7
10.5	6.5	8.7	1.3	4.9
12	7	9.8	1.4	5.0
13.5	7.5	10.9	1.5	5.2
15	8	12.0	1.5	5.3
16.5	8.5	13.0	1.5	5.6
18	9	14.3	1.6	5.7
19.5	9.5	15.6	1.6	5.8
21	10	16.8	1.7	6.0
22.5	10.5	18.2	1.7	6.1
24	11	19.6	1.8	6.2
25.5	10.5	18.2	1.7	6.1
27	10	16.9	1.7	5.9
28.5	9.5	15.5	1.6	5.8
30	9	14.2	1.6	5.7
31.5	8.5	12.9	1.5	5.6
33	8	11.7	1.5	5.5
34.5	7.5	10.5	1.4	5.4
36	7	9.4	1.3	5.2
37.5	6.5	8.3	1.3	5.1
39	6	7.3	1.2	4.9
40.5	0	0	0	-

2.2. Microchannel test section and the self-rewetting fluids

The microchannel test section was comprised of five microchannel arrays with different features and

designs. We used an array of 32 interconnected microchannels with a cross-section of 50×50 μm with a borosilicate glass covering the upper side of the silicon. The temperature sensors and the heater were positioned at the bottom side of the microchannel array, which is schematically presented in figure 2. All of the walls and bottom of the microchannels were smooth after the etching process with the roughness well below 1 μm, and more importantly no artificial nucleation cavities were added.

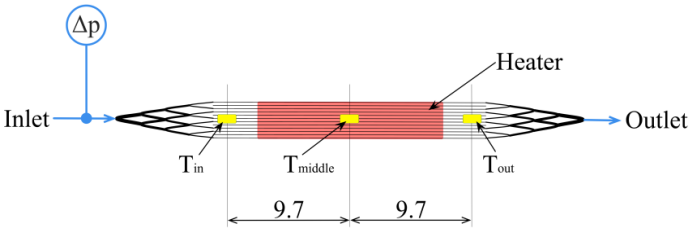

Figure 2. Array of microchannels.

The maximal solubility of long chain alcohols was found in the open literature, however the solubilities were not unambiguously defined. The ranges of maximal solubilities of alcohols in water at 25°C are presented in table 2. The weight concentrations of alcohols used in our experimental work were fixed at approximately 80 % of the average maximal solubility at 25°C found in Yalkowsky *et al* [19]. Therefore, the mass concentrations of aqueous solutions of 1-butanol, 1-pentanol, 1-hexanol and 1-heptanol were 6.0%, 2.0%, 0.60% and 0.15%, respectively.

Table 2. The solubility of alcohols in water.

Alcohol	Lowest solubility (g/L)	Lowest solubility (wt%)	Largest solubility (g/L)	Largest solubility (wt%)	Average maximal solubility (wt%)	Used concentration (wt%)
1-butanol	65	6.52	83	8.32	7.42	6.0
1-pentanol	17	1.71	33	3.31	2.51	2.0
1-hexanol	5.8	0.58	9.1	0.91	0.75	0.60
1-heptanol	1.7	0.17	1.8	0.18	0.18	0.15

3. Results and discussion

3.1. Acquired experimental data and visualization

The volumetric flow of the working fluid was fixed at 0.5 mL/min and 1 mL/min, which corresponds to the mass flux of 104 kg/m^{2}s and 208 kg/m^{2}s, respectively. The effectiveness of heat transfer is commonly evaluated with three parameters: the heat transfer coefficient (HTC), the critical heat flux (CHF), and the superheat needed for the onset of boiling (ONB). The comparative analysis of various working fluids presented in this paper was focused primarily on the ONB. The gauge pressure measurements allow a distinct determination of boiling incipience, as it is seen in the figure 3. The summary of the pressure and temperature measurements at the ONB is given in table 3, as the actual values are difficult to obtain from the figures included. The maximum temperature was measured in the middle of microchannels at all experimental runs. Lower temperature of the ONB corresponds well with a lower gauge pressure after the boiling incipience at both volumetric flows for all working fluids.

The lowest temperatures of the ONB were measured with pure water as the working fluid at both analyzed volumetric flows. The pressure drop is lowering gradually with the increase of the fluid temperatures, whereas a sharp increase of the pressure occurs at the ONB due to the vapor backflows. At the volumetric flow of 0.5 mL/min the ONB was seen at first in water (102°C), and followed by hexanol (103°C), heptanol (108°C), pentanol (133°C) and butanol (133°C) aqueous solution.

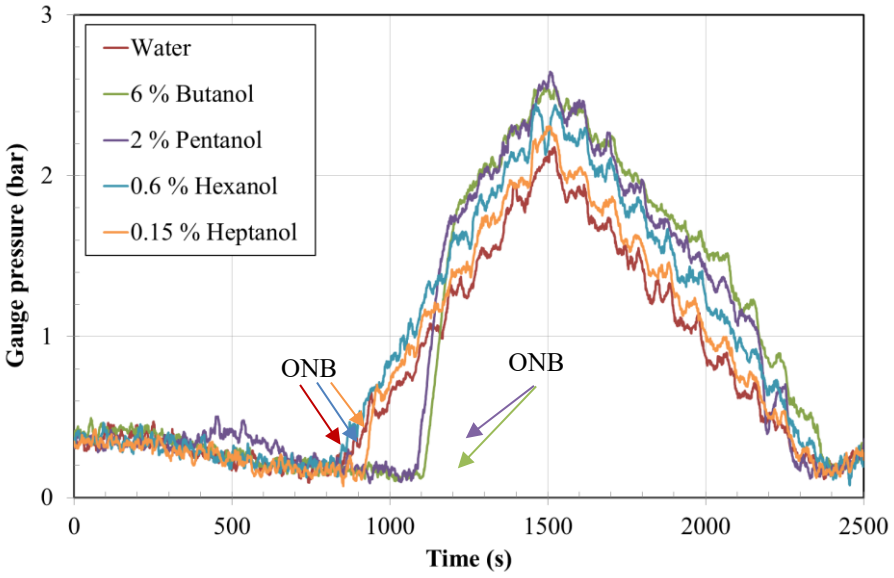

Figure 3. Gauge pressure at the volumetric flow of 0.5 mL/min.

Table 3. The summary of pressures and temperatures at the onset of boiling in microchannels.

	Maximum temperature at ONB (°C)		**Gauge pressure prior to ONB (bar)**		**Gauge pressure after ONB (bar)**	
Volumetric flow	0.5 mL/min	1 mL/min	0.5 mL/min	1 mL/min	0.5 mL/min	1 mL/min
Water	102	105	0.17	0.50	0.37	0.69
6% butanol	133	163	0.13	0.30	1.83	2.92
2% pentanol	131	129	0.16	0.33	1.73	2.02
0.6% hexanol	103	136	0.14	0.28	0.43	2.09
0.15% heptanol	108	108	0.13	0.38	0.66	0.79

Elevated temperatures of the ONB resulted in larger pressure jump. It can be derived from the table 3 that the pressure has risen for a factor of 2.2 at water and for a factor of 14.1 at the butanol solution, which is proportional to the superheat needed for commencement of boiling. The measured pressures presented in figure 3 show that the pressure drop of water was lower at almost all times and temperatures. Therefore, the surface of the microchannels was not appropriate for boiling of SRF. Firstly, the superheat needed for the ONB was higher for all of the SRFs used and secondly, the pressure drop during boiling was the lowest when water was used, which implicates that the boiling surface encouraged abrupt bubble nucleation of the SRFs.

The temperatures at the inlet, middle and outlet of the microchannels are presented in figures 4(a)-4(c), respectively. The temperatures at the middle of the microchannels were the highest, followed by the outlet and the inlet temperatures. Distinctive differences in temperatures are seen at the ONB, as the single-phase liquid flow transfers heat substantially less effective as the two-phase flow. Consequentially, the temperature plunges at the boiling incipience. Some differences are also seen during boiling of pentanol aqueous solution at 2200 s. This is the result of a more vigorous boiling of the SRF, which momentarily reduces the upstream temperatures.

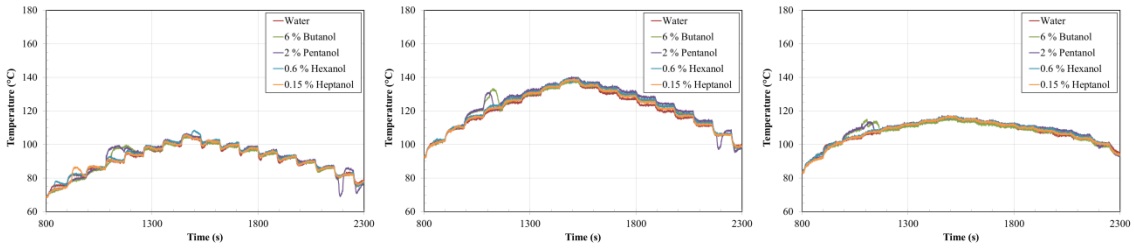

(a) (b) (c)

Figure 4. Temperatures at the (a) inlet; (b) middle and (c) outlet of the microchannels at 0.5 mL/min.

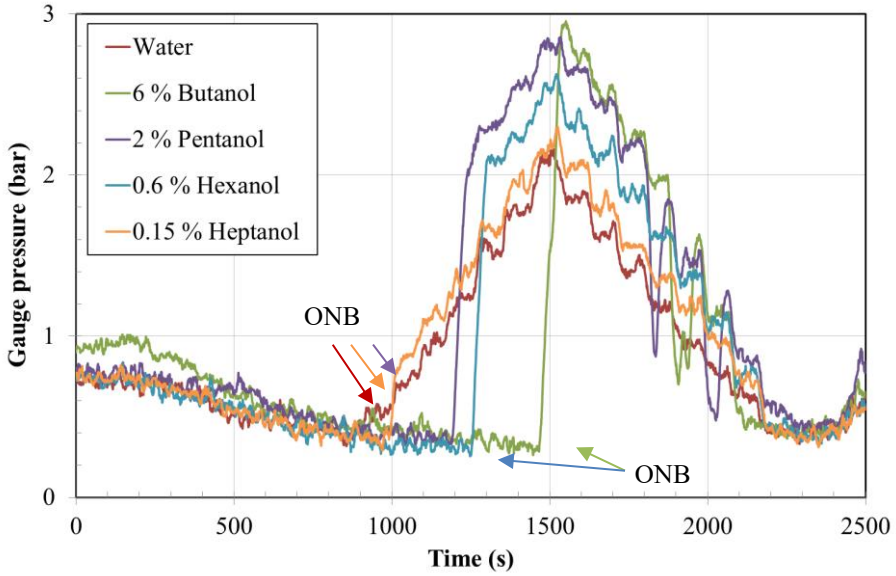

Figure 5. Gauge pressure at the volumetric flow of 1 mL/min.

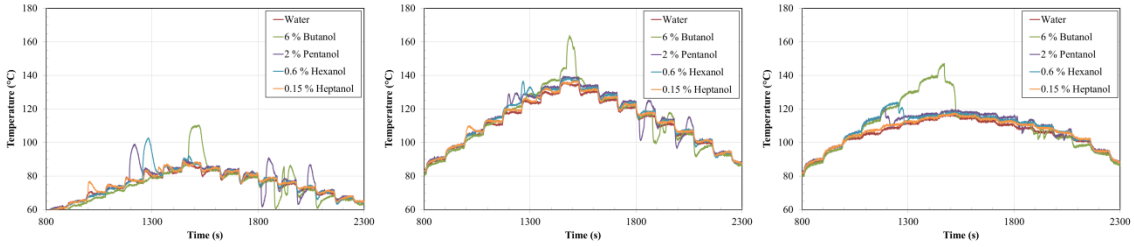

(a) (b) (c)

Figure 6. Temperatures at the (a) inlet; (b) middle and (c) outlet of the microchannels at 1 mL/min.

Similar results were measured at the larger volumetric flow of 1 mL/min, as it is seen from figures 5 and 6. The ONB was achieved in water at 105°C, heptanol solution at 108°C, pentanol solution at 129°C, hexanol solution at 136 °C and butanol solution at 163°C. The pressure drop at ONB has risen from 0.50 bar to 0.69 bar for water and from 0.30 bar to 2.92 bar for 6% butanol solution. The pressures were again the lowest when water was used as the working fluid, whereas the butanol and pentanol solutions show severe pressure fluctuations during the decrease of the heating power. This phenomenon is visually seen as an abrupt boiling of a mist like two-phase flow, which occurs due to the highly superheated smooth surface.

The temperatures at the inlet, middle and outlet of the channels are presented in figures 6(a)-6(c).

The distinctive temperature differences are seen at the ONB, when pentanol, hexanol and especially butanol solution were used as the working fluids. The temperature of the boiling incipience was 163°C for the butanol solution, whereas pure water started boiling at merely 105°C at the same volumetric flow and the same microchannel array. The absence of artificial nucleation cavities was the origin of the high superheat needed for the ONB of the butanol solution, as its surface tension is much lower compared to water. The addition of long-chain alcohols lowered the contact angle on the silicon, which postponed the boiling commencement at all the SRFs used. The temperature measurements further indicate the presence of an abrupt nucleation and vigorous boiling, which is more pronounced during butanol and pentanol solution boiling at a decreasing heat flux. The temperatures were oscillating up to 30°C during a constant heating power. The temperature fluctuations are less distinctive at the outlet, as there was mostly vapor present for all of the working fluids. The upstream portion of the microchannels were filled mostly with liquid water, hexanol or heptanol solutions, whereas the same location contained a vapor-liquid mixture of pentanol or butanol solutions during the temperature oscillations in the range of 1800 s to 2100 s.

Sample images during flow boiling of water and 6% butanol solution boiling are presented in figure 7. The sets of images that were selected from 4000 fps high-speed videos are depicting the most distinctive differences between the boiling phenomenon of water and SRFs in the microchannel array without any artificially etched nucleation cavities. The boiling of water was stable without any abrupt occurrences, whereas the boiling of the butanol solution displays an eruptive boiling behavior, which results in a mist two-phase flow with high pressure and temperature oscillations.

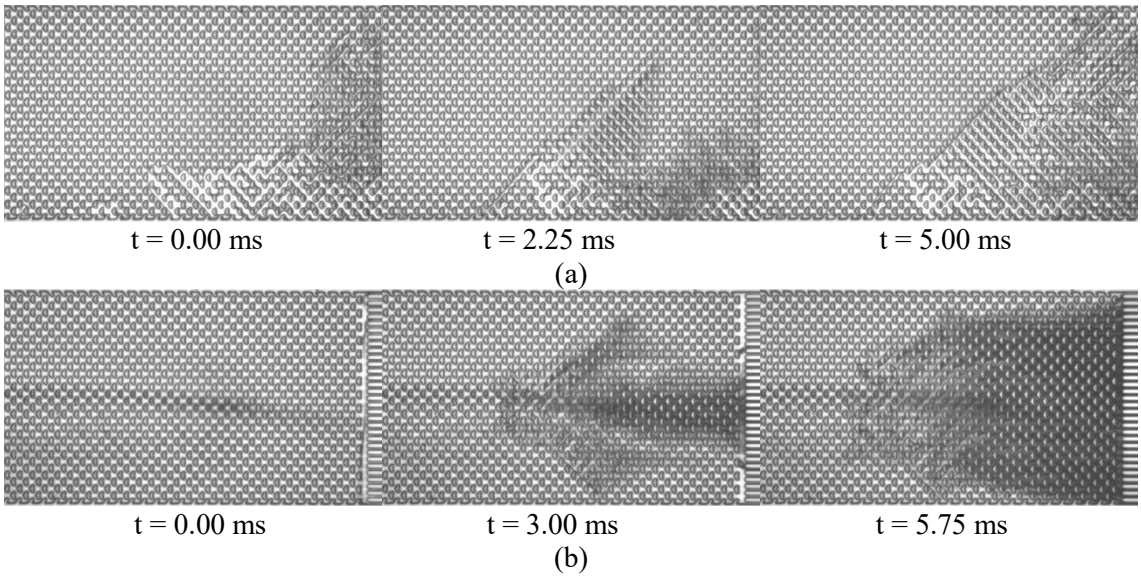

Figure 7. Flow boiling of (a) pure water and (b) 6 % aqueous butanol solution at 1 mL/min and 15.6 W.

3.2. Wettability of the working fluids

The wettability of a fluid is highly dependent on the exact type of material and the actual surface topography. Wettability itself was already proven to have significant effect on pool boiling and flow boiling performance [20,21]. For that reason, we have performed the measurements of static and dynamic contact angles for all the working fluids on a silicon wafer. Dynamic contact angles are especially important, since the three-phase contact line around which high heat transfer occurs, is constantly advancing and receding during the boiling process. The contact angle measurements were performed at 25°C on goniometer equipped with a high-speed video camera, a microscopic objective and micrometer syringe with a steel size 22 capillary tube. The droplet volumes for static measurements were constantly 5 μL. Advancing and receding contact angles were measured as the

maximum and the minimum contact angles while adding or removing the fluid from the surface, respectively. The measured values of the contact angles presented in table 4 and figure 8 are the averaged values of ten measurements, whereas one sample image for each contact angle and fluid is additionally given in figure 8.

Table 4. The average values of static, advancing and receding contact angle.

	Static contact angle (°)	**Advancing contact angle (°)**	**Receding contact angle (°)**
Water	44	54	30
6% butanol	31	44	9
2% pentanol	38	50	11
0.6% hexanol	40	53	14
0.15% heptanol	43	54	12

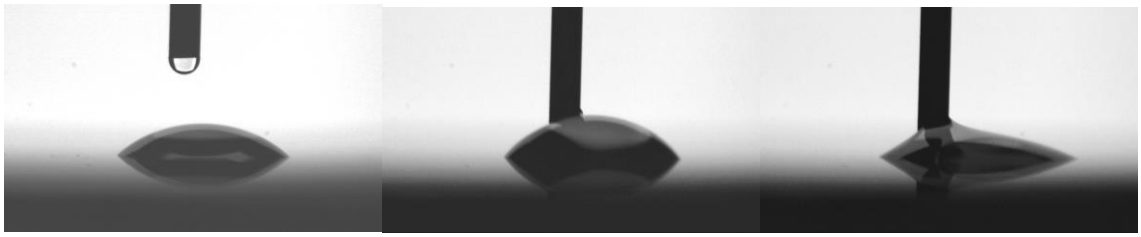

$\varphi_{static} = 44°$ $\varphi_{advancing} = 54°$ $\varphi_{receeding} = 30°$

(a)

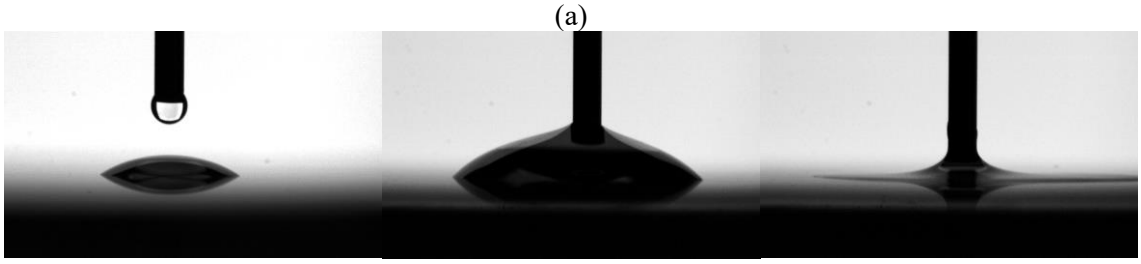

$\varphi_{static} = 31°$ $\varphi_{advancing} = 44°$ $\varphi_{receeding} = 9°$

(b)

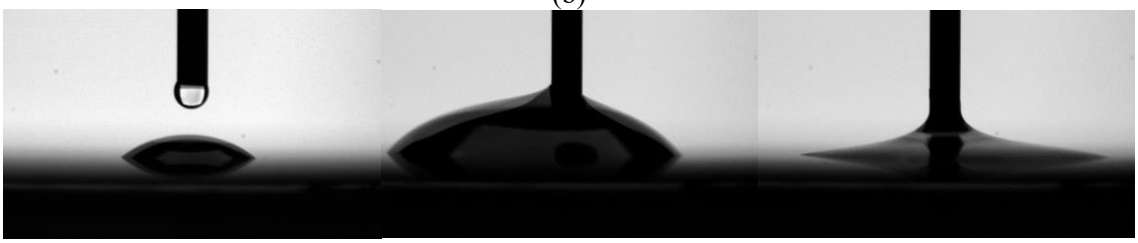

$\varphi_{static} = 38°$ $\varphi_{advancing} = 50°$ $\varphi_{receeding} = 11°$

(c)

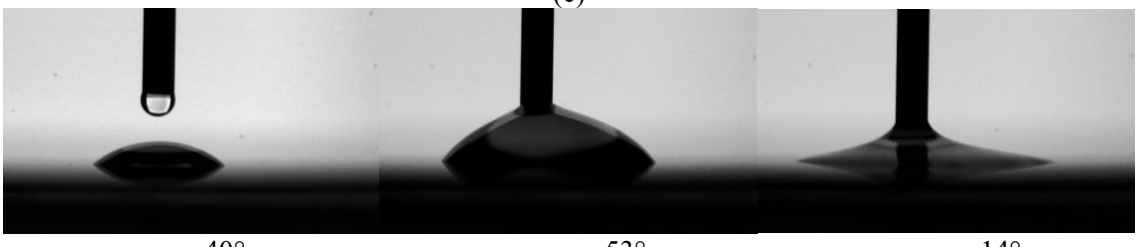

$\varphi_{static} = 40°$ $\varphi_{advancing} = 53°$ $\varphi_{receeding} = 14°$

(d)

$\varphi_{static} = 43°$ $\varphi_{advancing} = 54°$ $\varphi_{receeding} = 12°$

(e)

Figure 8. Static and dynamic contact angles of (a) water, (b) 6% butanol, (c) 2% pentanol, (d) 0.6% hexanol and (e) 0.15% heptanol solution on a silicon wafer.

The largest contact angles were measured at a water drop placed on the silicon wafer, whereas the lowest angles were determined for the 6% butanol solution. The contact angles of all the other analyzed SRFs were measured between these two outermost angles. The wettability results were anticipated on the basis of temperature and pressure measurements at the ONB. Namely, the larger contact angle of the fluids on the silicon surface coincide extremely well with the lower superheat needed for the boiling incipience.

4. Conclusions

The presented experimental results show that the onset of nucleate boiling was postponed to higher temperatures for the self-rewetting fluids. The superheats required for the ONB were up to 57 K higher for the 6% aqueous butanol solution compared to pure water. The temperature of the ONB for other investigated SRFs (2% pentanol, 0.6% hexanol and 0.15% heptanol solution) increased as well, however it was less pronounced in comparison with the butanol solution. The comparative analysis of the working fluids is consistent at both employed mass fluxes of 104 kg/m^{2}s and 208 kg/m^{2}s. The most probable origin of the boiling suppression is the combination of smooth surfaces and lower surface tension of the SRFs compared to water. Results showed that 6% butanol solution provides the lowest static and dynamic contact angles among all the tested fluids. The wall temperatures decreased substantially after the incipience of boiling, as the heat transfer coefficient increased at the single-phase to two-phase flow transition. The temperature drop and the rise of the pressure were well pronounced in the experiments performed, due to the interconnected microchannels in the arrays, which promoted the propagation of boiling to a larger surface of the microchannels. Consequentially, the temperatures dropped up to 25 K and the pressure has risen up to 14 times at the ONB. The comparative analysis of various working fluids was enabled with the utilization of same heating procedure for all of the experimental runs. Therefore, the temperature time dependence was measured at approximately the same heating power and heat losses for all of the fluids. The analyzed temperatures after the incipience of boiling indicate that pure water was transferring heat superiorly compared to the SRFs. Although the positive surface gradient of the SRFs improves the wettability of the dried areas, it was not the deciding factor for an improved heat transfer during flow boiling. The visualization of the boiling phenomenon revealed that the SRFs were boiling abruptly in an oscillating mist like two-phase flow. The most probable cause of the deteriorated boiling heat transfer is the absence of properly sized nucleation sites, which would stabilize the two-phase flow.

The presented study demonstrated that the introduction of SRFs to a microchannel heat transfer device has some pitfalls, which should be recognized and mitigated already at the design phase of the microchannel fabrication. The combination of the working fluid and microchannel surface is crucial not only for an earlier transition to boiling, but also for a more stable and efficient nucleation of bubbles. In the opposite case, the temperatures of the ONB are higher and the following flow boiling becomes more unstable, vigorous and abrupt, which introduces high temperature and pressure fluctuations.

References

[1] Kandlikar S G, Colin S, Peles Y, Garimella S, Pease R F, Brandner J J and Tuckerman D B 2013 Heat transfer in microchannels—2012 status and research needs *J Heat Transfer* **135** 091001-01-18
[2] Sitar A and Golobic I 2016 Effect of nucleation cavities on enhanced boiling heat transfer in microchannels *Nanosc Microsc Therm* **20** 33-50
[3] Kuo C J and Peles Y 2007 Local measurement of flow boiling in structured surface microchannels *Int J Heat Mass Transfer* **50** 4513-26
[4] Wang G, Cheng P and Bergles A E 2008 Effects of inlet/outlet configurations on flow boiling instability in parallel microchannels *Int J Heat Mass Transfer* **51** 2267-81
[5] Lee J Y, Kim M-H, Kaviany M and Son S Y 2011 Bubble nucleation in microchannel flow boiling using single artificial cavity *Int J Heat Mass Transfer* **54** 5139-48
[6] Law M, Lee P-S and Balasubramanian K 2014 Experimental investigation of flow boiling heat transfer in novel oblique-finned microchannels *Int J Heat Mass Transfer* **76** 419-31
[7] Ghaedamini H, Salimpour M R and Campo A 2011 Constructal design of reverting microchannels for convective cooling of a circular disc *Int J Therm Sci* **50** 1051-61
[8] Petkovsek J, Heng Y, Zupancic M, Gjerkes H, Cimerman F and Golobic I 2016 Ir thermographic investigation of nucleate pool boiling at high heat flux *Int J Refrig* **61** 127-39
[9] Savino R, Cecere A and Di Paola R 2009 Surface tension-driven flow in wickless heat pipes with self-rewetting fluids *Int J Heat Fluid Fl* **30** 380-8
[10] Senthilkumar R, Vaidyanathan S and Balasubramanian S 2011 Thermal analysis of heat pipe using self rewetting fluids *Therm Sci* **15** 879-88
[11] Wu S-C 2015 Study of self-rewetting fluid applied to loop heat pipe *Int J Therm Sci* **98** 374-80
[12] Su X, Zhang M, Han W and Guo X 2016 Experimental study on the heat transfer performance of an oscillating heat pipe with self-rewetting nanofluid *Int J Heat Mass Transfer* **100** 378-85
[13] Hu Y, Zhang S, Li X and Wang S 2014 Heat transfer enhancement mechanism of pool boiling with self-rewetting fluid *Int J Heat Mass Transfer* **79** 309-13
[14] Hu Y, Zhang S, Li X and Wang S 2015 Heat transfer enhancement of subcooled pool boiling with self-rewetting fluid *Int J Heat Mass Transfer* **83** 64-8
[15] Zhou L, Wang Z, Du X and Yang Y 2015 Boiling characteristics of water and self-rewetting fluids in packed bed of spherical glass beads *Exp Therm Fluid Sci* **68** 537-44
[16] Zhou S, Zhou L, Du X and Yang Y 2017 Heat transfer characteristics of evaporating thin liquid film in closed microcavity for self-rewetting binary fluid *Int J Heat Mass Transfer* **108A** 136-45
[17] Sitar A and Golobic I 2015 Heat transfer enhancement of self-rewetting aqueous n-butanol solutions boiling in microchannels *Int J Heat Mass Transfer* **81** 198-206
[18] Sitar A, Sedmak I and Golobic I 2012 Boiling of water and fc-72 in microchannels enhanced with novel features *Int J Heat Mass Transfer* **55** 6446-57
[19] Yalkowsky S H, He J and Jain P 2010 *Handbook of Aqueous Solubility Data* 2nd Ed. (Boca Raton, FL, USA: CRC Press)
[20] Shojaeian M and Koşar A 2015 Pool boiling and flow boiling on micro- and nanostructured surfaces *Exp Therm Fluid Sci* **63** 45-73
[21] Bourdon B, Di Marco P, Rioboo R, Marengo M and De Coninck J 2013 Enhancing the onset of pool boiling by wettability modification on nanometrically smooth surfaces *Int Commun Heat Mass Transfer* **45** 11-5